TOWARDS COMPREHENSIVE VARIATION MODELS FOR DESIGNING VEHICLE MONITORING SYSTEMS *

Daniel A. McAdams, Ph.D.
Dept. of Mechanical & Aerospace Eng.
Engineering Mechanics
University of Missouri-Rolla
Rolla, Missouri 65409-0050
Phone: 573 341 4494
Email: dmcadams@umr.edu

Irem Y. Tumer, Ph.D.
Computational Sciences Division
MS 269-3
NASA Ames Research Center
Moffett Field, California 94035
Phone: 650 604 2976
Email: itumer@mail.arc.nasa.gov

Abstract

When designing vehicle vibration monitoring systems for aerospace devices, it is common to use well-established models of vibration features to determine whether failures or defects exist. Most of the algorithms used for failure detection rely on these models to detect significant changes in a flight environment. In actual practice, however, most vehicle vibration monitoring systems are corrupted by high rates of false alarms and missed detections. This crucial roadblock makes their implementation in real vehicles (e.g., helicopter transmissions and aircraft engines) difficult, making their operation costly and unreliable. Research conducted at the NASA Ames Research Center has determined that a major reason for the high rates of false alarms and missed detections is the numerous sources of statistical variations that are not taken into account in the modeling assumptions.

In this paper, we address one such source of variations, namely, those caused during the design and manufacturing of rotating machinery components that make up aerospace systems. We present a novel way of modeling the vibration response by including design variations via probabilistic methods. Using such models, we develop a methodology to account for design and manufacturing variations, and explore the changes in the vibration response to determine its stochastic nature. We explore the potential of the methodology using a nonlinear cam-follower model, where the spring stiffness values are assumed to follow a normal distribution. The results demonstrate initial feasibility of the method, showing great promise in developing a general methodology for designing more accurate aerospace vehicle monitoring systems.

*Submitted for Review, ASME Journal of Mechanical Design. Conference version published in DETC 2002 (DETC2002-DFM34161).

1 Designing Vehicle Monitoring Systems

This work addresses a need to design effective vehicle health monitoring systems for aerospace vehicles. Ongoing research focuses on various sources of variation that result in unexpected performance variations. The current focus is in assuring that correct models of system input signals are used for the algorithms and metrics used for failure detection. This paper explores one aspect of modeling input signals in such systems, namely, the consideration of design and manufacturing variations for the system response variable that is being monitored, namely, the vibration signature.

In the following subsections, we first present some backgound research on vehicle health monitoring systems, two examples of the types of variations encountered in such systems, and discuss the need to incorporate probabilistic models to account for such variations. Then, the use of probabilistic methods (e.g., Monte Carlo simulation) is explored with a simple example in design, and compared to more traditional variation analysis techniques. Next, a lumped parameter dynamic model is presented for a complex cam-follower system used in this paper, followed by an analysis of vibration data obtained from such a model. Finally, the Monte Carlo simulation technique is used to vary a subset of the design parameters. The effect on the vibration response is explored to determine whether probabilistic methods can be used to model the inherent variations observed in the dynamic response of complex systems.

1.1 Background and Objective

Failures in rotating machinery for high-risk aerospace applications are unacceptable when they result in catastrophic accidents, and undesirable when they result in high maintenance costs. In an attempt to detect any anomalous behavior during flight for increased safety, most aircraft manufacturers and operators are moving towards installing vehicle health monitoring systems. Despite the motivation to make these systems standard onboard aircraft, false alarms and missed detections still remain a serious concern, making their reliability questionable and their operation costly in practice. One of the main reasons for the high rate of false alarms and missed failures is the lack of a statistically sufficient sample of baseline and failure signatures from which generalizations can be made. Specifically, since failure events are rare in such highly-maintained systems, there is no knowledge of the distribution of responses they could generate.

Recent work at NASA Ames Research Center has demonstrated that the statistical variations in baseline (healthy) data must be accounted for to assure accurate anomaly detection in aircraft monitoring systems (Huff et al., 2000; Huff et al., 2002; Tumer and Huff, 2002; Tumer and Huff, 2001). In this work, we address the mismatch between modeled responses and empirical observations by developing statistically-accurate models that take variations into account. The specific objective is to explore probabilistic approaches to generate a reliable distribution of vibration responses using lumped-parameter dynamic models. If such an approach proves feasible, more accurate models of healthy and faulty aircraft vibration data will be developed and used as signal models for vibration monitoring systems.

1.2 Observed Variations in Vibration Signatures

For rotating machinery, vibration signals are thought to contain indicators of defects and usage damage in rotating components such as gears, bearings, shafts, rotors, etc. Each of the rotating components emanate specific frequencies that appear in the vibration signals; any changes in the amplitude and frequency content of these signatures, or the occurrence of sidebands or additional frequencies, is indicative of potential variations and defects. The types of variations of interest in this work include those that are inherent from the design and manufacturing processes (e.g., tolerances, assembly variations, surface roughness and waviness errors), material defects, cracks, and other point defects on the rotating components (Tumer and Huff, 2001; Huff et al., 2002; Tumer and Huff, 2002). In this paper, we focus on variations introduced during design and manufacturing, effectively introducing a stochastic nature to the modeling parameters such as stiffness, mass, and damping.

Examples of design, manufacturing, and assembly variations having significant impact on system vibrations signals have been found throughout our research. As a first example, Figure 1 shows a schematic of a helicopter transmission for an OH58 helicopter (Lewicki and Coy, 1987), as well as a plot of experimental data we have collected using a test rig which houses such a transmission box (Huff et al., 2000). The different lines correspond to four different assembly instances of the same transmission box. Vibration data were collected for each assembly instance. Within each instance, three variables were varied (namely torque, mast lift and mast bending forces) using a factorial experimental design. As shown, the overall vibration levels (total power) varied significantly depending on the test conditions defined by the four experimental variables (Huff et al., 2000).

As a second example, Figure 2 shows a theoretical plot of the frequency spectrum from one of the gear systems contained in the helicopter transmission, based on our empirical observations (Huff et al., 2002). The geometry of the gear system (epicyclic gears) includes four smaller gears (planet gears) revolving around a larger gear (sun gear) (Smith, 1999). In this example, the theoretical epicyclic gear mesh frequency for a single planet would fall on 99 in the x-axis (equal to the number of teeth), as shown in black in Figure 2, followed by a set of harmonics. For a more realistic system, the exact epicyclic gear mesh frequency appears at frequencies clustered around the theoretical frequency value due to the spacing variations between planet gears. Figure 2 shows the frequency clustering for two sets of equally-spaced planet gears (shown in red), as opposed to four equally-spaced planet gears (shown in blue). The spacing between the planet gears is subject to design variations, which result in the observed difference in frequency distributions, which in turn can invalidate the signal modeling assumptions (Huff et al., 2002).

1.3 Probabilistic Variation Analysis in Design

A significant degree of variation is introduced during the design, manufacturing, and assembly of components that make up aircraft systems. Standard tolerance variation analysis methods used in design address this variability by predicting the total variation in the final system (Creveling, 1997). Because we are starting from similar variation

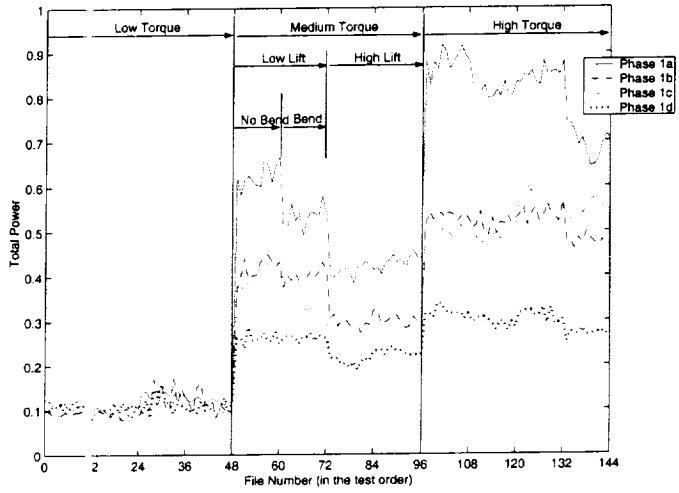

Figure 1: Variations in Vibration Levels in a Rotorcraft Transmission.

sources, this approach will be explored and extended here to dynamic models of complex systems to predict the variation in vibration response characteristics.

A simple mechanical assembly is shown in Figure 3, where three rectangular blocks of dimension X_1, X_2, and X_3 are designed and manufactured to fit within the allowable space of dimension Y. Due to the inherently probabilistic nature of the manufacturing process, each of the dimensions is assigned specific tolerances based on a distribution set by the designer (either based on empirical manufacturing data or process capability specifications (Creveling, 1997).) Typically, statistical tolerance analysis techniques are applied to geometric models of such assemblies to predict the magnitude and range of the variations in critical assembly features. For example, a Monte Carlo simulation approach is shown in Figure 3 to perform tolerance analysis for each manufacturing and design parameter (Hammersley and Handscomb, 1964; Creveling, 1997). Values of each parameter X_i are drawn randomly from an assumed distribution function, and then combined through a functional model to determine the corresponding values for the final variable of interest. The statistical moments are then computed for the resultant values, which in turn are used to determine the probability distribution that matches the final assembly variable Y.

2 Monte Carlo Methods: Summary and Example

In this paper, we explore the application of Monte Carlo methods to variation modeling for the purpose of determining performance limits of complex dynamic systems. This section presents the fundamentals of such an approach using a simple design example.

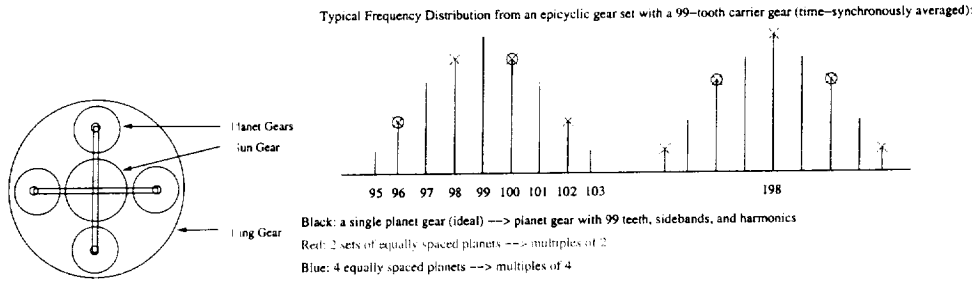

Figure 2: Variations in the Frequency Response in Epicyclic Gears.

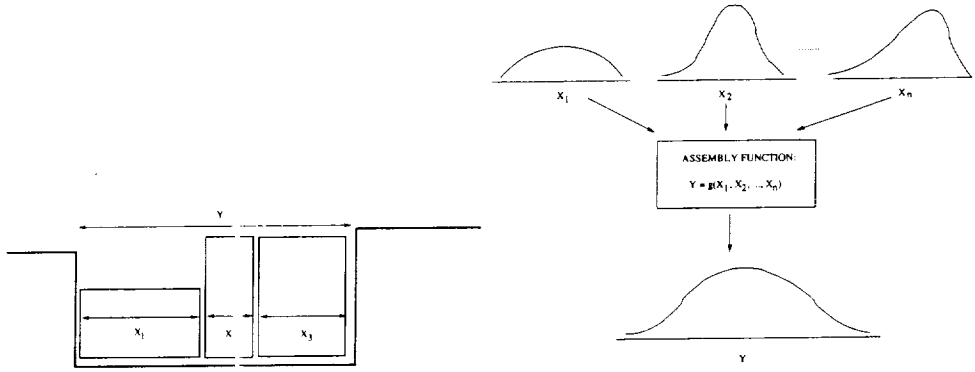

Figure 3: Application of Statistical Methods to Tolerancing.

Conceptually, Monte Carlo simulation is simple and elegant (Metropolis and Ulam, 1949; Hammersley and Handscomb, 1964). Consider some function

$$y = f(x_1, x_2, ..., x_n), \tag{1}$$

where y is a known function of random variables $x_1, x_2, ..., x_n$. We assume that each x_i has a known random nature and all the x_i's are statistically independent. The question we wish to answer (or simulate) is: what is the random nature of y?

To determine the random nature of y, a random sample is generated for each x_i. Using the known function f (some system/performance model), y is generated next. Depending on the information needed from the random nature of y (perhaps a mean μ and standard deviation σ, or the number of times y exceeds some value out of 1000 trials, etc.) the value of y or some sort of frequency count is recorded.

As an example, consider the design of a helical coil spring to achieve some specific spring constant k. The relation

between the performance parameter k and the design variables is

$$k = \frac{d^4 G}{8D^3 N}, \tag{2}$$

with d the wire diameter out of which the spring is made, G the shear modulus of the spring material, D the diameter of the spring (helix diameter), and N the total number active turns or coils of the spring. As a first pass, a deterministic model with $d = 1.5\ mm$, $G = 79\ GPa$, $D = 18.0\ mm$, and $N = 13$ turns gives $k = 660 N/m$. In reality, the values of d, G, D, and N do not always take on the same precise values for each spring that is manufactured. Thus, a more accurate (with regard to how well it represents reality) design model would be one which considers the way the variations of d, G, D, and N cause a variation in k.

For cases where the function f is simply represented and smooth enough to provide second derivatives, a low-order Taylor series approximation for the mean of y can be expressed as below, with the partial derivatives evaluated at $x_i = \mu_i$ (Hahn and Shapiro, 1994; McAdams and Wood, 2000):

$$\mu_y = f(\mu_{x_1}, \mu_{x_2}, \ldots, \mu_{x_n}) + \frac{1}{2}\sum_{i=1}^{n} \frac{\partial^2 f}{\partial x_i^2} Var(x_i). \tag{3}$$

Similarly, a low-order approximation for the variance of y can be expressed as:

$$Var(y) = \sum_{i=1}^{n} \left(\frac{\partial f}{\partial x_i}\right)^2 Var(x_i). \tag{4}$$

Equations (3) and (4) can be applied to Eq. (2) to yield:

$$\begin{aligned} \mu_k &= \frac{\mu_d{}^4 \mu_G}{8\mu_D{}^3 \mu_N} + \frac{1}{2}\frac{12\mu_d{}^2 \mu_G}{8\mu_D{}^3 \mu_N} Var(d) \\ &+ \frac{1}{2}\frac{12\mu_d{}^4 \mu_G}{8\mu_D{}^5 \mu_N} Var(D) + \frac{1}{2}\frac{2\mu_d{}^4 \mu_G}{8\mu_D{}^3 \mu_N{}^2} Var(N), \end{aligned} \tag{5}$$

and,

$$\begin{aligned} Var(k) &= \left(\frac{4\mu_d{}^3 \mu_G}{8\mu_D{}^3 \mu_N}\right)^2 Var(d) + \left(\frac{\mu_d{}^4}{8\mu_D{}^3 \mu_N}\right)^2 Var(G) \\ &+ \left(\frac{-3\mu_d{}^4 \mu_G}{8\mu_D{}^4 \mu_N}\right)^2 Var(D) + \left(\frac{-\mu_d{}^4 \mu_G}{8\mu_D{}^3 \mu_N{}^2}\right)^2 Var(N). \end{aligned} \tag{6}$$

Substituting $d = 1.5\ mm$, $G = 79\ GPa$, and $D = 18.0\ mm$ for the average values μ_d, μ_G, μ_D, μ_N and taking $Var(d) = 2.5 \times 10^{-5}\ mm$, $Var(G) = 6.9\ GPa$, $Var(D) = 18.6 \times 10^{-3}\ mm$, and $Var(N) = 1.87 \times 10^{-3}$ turns (Shigley and Mischke, 2001) for the variations gives $\mu_k = 560\ N/m$ and $Var(k) = 27{,}600\ N/m$. Translating this into a mechanical tolerance using a common convention assuming a random variable (i.e., tolerances $= 3\sigma_x = 3\sqrt{(Var(x))}$) gives $498\ N/m$.

Using Eqs. (3) and (4) allows designers a starting point to understand, and compensate or *design* for, the effects of variation. Nevertheless, this approximate approach has a number of key shortcomings that become apparent and critical as we explore more complex systems and the compound effects of different types of variation. Of critical importance here are that: a) as engineering models become complex and computational, Eqs. (3) and (4) fail to provide tractable analysis, and b) these two equations give us limited, and at times misleading, information about the probability distribution function of y. As an example, consider the relation $y = sin(x)$. Using Eqs. (3) and (4), and

taking x to be a random variable from a standard normal distribution gives $\mu_y = 0$ and $\sigma_y = 1$. Such a result may lead a designer to the notion that y can be modeled as a variable from a standard normal distribution. If this notion were used to make parameter specifications or expectations of failure, important errors could occur. Shown in Fig. 4 is a plot of the probability density function of y. The probability density function for y is determined by applying a coordinate transformation theorem from statistics (Eisen, 1969). A key restriction of this theorem is that the mapping of $y = f(x)$ be one to one, which is violated in our simple spring example.

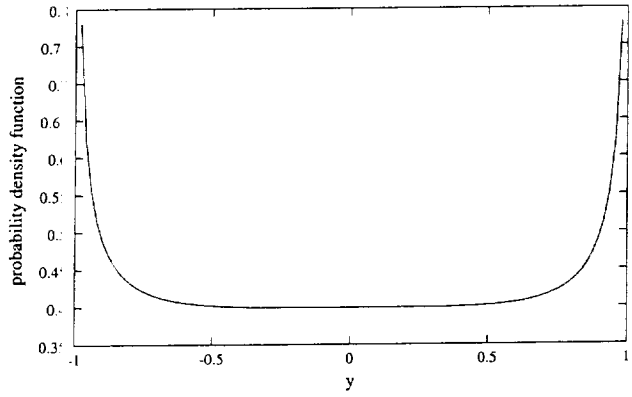

Figure 4: The pdf of y ($y = sin(x)$, x is a normal variable.)

Returning to the spring example, we now use Monte Carlo simulation to explore the variation in k as a function of the variations in d, G, D, and N. The histogram in Fig. 5 is generated performing a Monte Carlo simulation as outlined earlier in this section. Based on this simulation, there were no springs (out of a sample run of 100,000 springs) that fell below $k = 660 - 498\ N/m$ and above $k = 660 + 498\ N/m$ (taking the tolerance 498 N/m). This is compared to 270 (.27% from three-sigma tolerancing) if k were treated as a normally distributed random variable. The standard deviation of the Monte Carlo simulated springs is 17.5 N/m leading to a 3σ tolerance of 52.5 N/m. The significant difference between the Monte Carlo simulated variation and that approximated by Eq. 4 is due to the non-linearity of Eq. 2. Also, this comparison highlights the potential for engineering errors (in this case likely of a conservative nature) that would be made based on simple, linearized, analytic models such as those given by Eqs. 3 and 4.

This short review and comparison of approaches to represent variation in design and manufacturing highlights some of the potential advantages of Monte Carlo simulation. In summary, with the minimal penalty of some computation time, Monte Carlo simulation provides more useful information for the designer. Based on this insight, we use Monte Carlo simulation to explore how different sources of variation combine in more complex systems to influence the overall response and performance of a dynamic system.

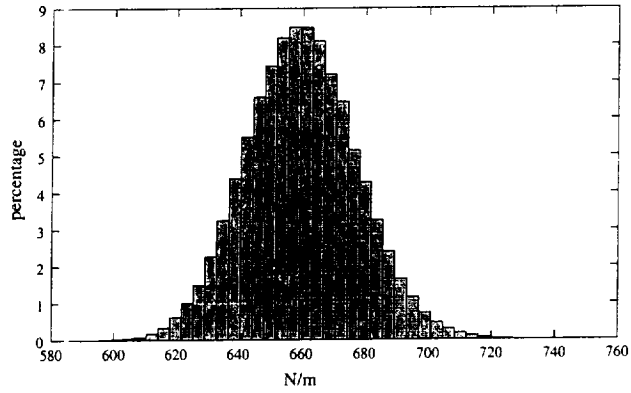

Figure 5: Histogram of k generated using Monte Carlo simulation.

3 Application: Cam-Follower Response

A lumped-parameter, seven degree-of-freedom (fourteenth-order) model of a cam follower is used in this paper as an example of a complex nonlinear system. The cam-follower system is shown in Figure 6(a), and a schematic of the model is shown in Figure 6(b), adapted from (Grewal and Newcombe, 1988) and (McAdams and Wood, 1996). The parameter values for the cam-follower system were taken from (Grewal and Newcombe, 1988), and are listed in Table 1. The equations of motion for the model are:

$$\begin{aligned} I_c\ddot{\theta} &= -C_{sf}(\dot{\theta}_c - \dot{\theta}_i) - K_{sf}(\theta_c - \theta_i) \\ &\quad -C_b\dot{\theta}_c - T_c, \end{aligned} \tag{7}$$

$$\begin{aligned} M_c\ddot{y}_1 &= -C_{vs}\dot{y}_1 - K_{vs}y_1 - F_c\cos\Phi \\ &\quad +F_p, \end{aligned} \tag{8}$$

$$\begin{aligned} M_r\ddot{y}_2 &= -C_f(\dot{y}_2 - \dot{y}_3) - K_f(y_2 - y_3) \\ &\quad +F_c\cos\Phi - F_p, \end{aligned} \tag{9}$$

$$\begin{aligned} M_f\ddot{y}_3 &= C_f(\dot{y}_2 - \dot{y}_3) + K_f(y_2 - y_3) \\ &\quad -C_4(\dot{y}_3 - \dot{y}_4) - K_4(y_3 - y_4) \\ &\quad -F_w - F_{cb}, \end{aligned} \tag{10}$$

$$\begin{aligned} M_3\ddot{y}_4 &= C_4(\dot{y}_3 - \dot{y}_4) + K_4(y_3 - y_4) \\ &\quad -C_3(\dot{y}_4 - \dot{y}_5) - K_3(y_4 - y_5), \end{aligned} \tag{11}$$

$$\begin{aligned} M_2\ddot{y}_5 &= C_3(\dot{y}_4 - \dot{y}_5) + K_3(y_4 - y_5) \\ &\quad -C_2(\dot{y}_5 - \dot{y}_6) - K_2(y_5 - y_6), \end{aligned} \tag{12}$$

and,

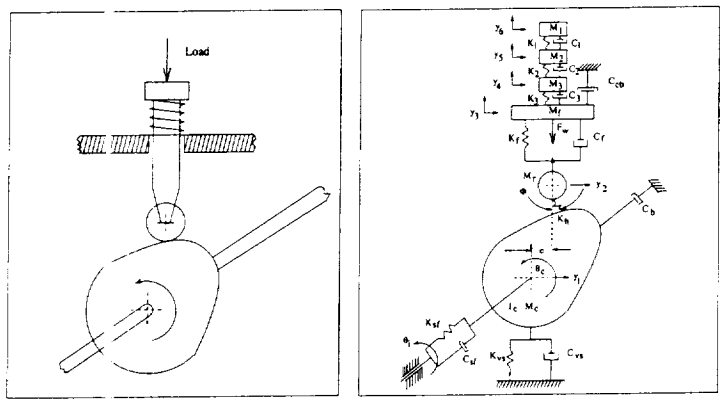

(a) Schematic. (b) The dynamic model.

Figure 6: Example: Cam-follower System.

$$\begin{aligned} M_1\ddot{y}_6 &= C_2(\dot{y}_5 - \dot{y}_6) + K_2(y_5 - y_6) \\ &\quad -C_1\dot{y}_6 - K_1 y_6, \end{aligned} \tag{13}$$

where θ_i is the input position, K_{sf} and C_{sf} model the damping and stiffness of the cam drive shaft, C_b accounts for friction losses in the drive shaft bearing, M_c is the mass of the cam itself, and I_c is the cam moment of inertia about its center of rotation. To account for the flexure of the shaft, a shaft stiffness, K_{vs}, and a damping, C_{vs} have been added. The offset of the cam follower from the center of the rotation of the cam is e, K_h accounts for deformation at the roller-cam interface, and M_r is the mass of the roller. The inertia of the roller is assumed to have a negligible effect on the rotational dynamics of the system. The mass of the follower is M_f, with K_f and C_f the structural stiffness and damping of the follower, respectively. C_{cb} accounts for the friction at the interface of the follower and the follower guide, F_{cb} is the force that results for this friction, and, F_w is the external load on the follower. The spring has been modeled as three elements to approximate the distributed mass of the spring. K_1, K_2, and K_3 are the distributed spring constants. The structural damping of the spring is approximated as C_1, C_2 and C_3. M_1, M_2, and M_3 are the mass of the spring. The state-space equations were integrated using a Runge-Kutta integration routine. A simple harmonic motion (SHM) cam profile with a maximum rise of $.0254m$ is used. The cam is assumed to rotate at a fixed rate of 1500 RPM (25 Hz). The numerical values for the constants used in the simulation of cam operation are presented in Table 1.

In Figure 7, the velocity and acceleration responses of the cam follower (from variable y_3 in Figure 6(b)) are shown. The dashed line shows the idealized follower velocities and accelerations as determined by differentiating the cam profile. The solid line shows the reality when system mass, stiffness, and the resulting dynamics are taken into consideration.

In contrast, Figure 8 shows the velocity and acceleration responses of the cam follower with a profile error of 25 μm

Table 1: Constant Values for the Cam-Follower Dynamic Model.

Element	Variable	Value
cam moment of inertia	I_c	$.00091034 kg/m^2$
cam shaft rotational damping	C_{sf}	$.01356 N \cdot m \cdot s/rad$
cam shaft rotational stiffness	K_{sf}	$22600 N \cdot m/rad$
drive shaft friction	C_b	$.113 N \cdot m \cdot s/rad$
cam mass	M_c	$.5017 Kg$
cam shaft horizontal damping	C_{vs}	$752.9 N \cdot s/m$
cam shaft horizontal stiffness	K_{vs}	$2.6e^9 N/m$
system preload	F_p	$266.62 N$
follower stiffness	K_f	$175.1e^6 N/m$
follower mass	M_f	$.340 kg$
follower damping ratio	η_f	.75
follower damping	C_f	$\eta_f 2\sqrt{M_f K_f}$
external follower load	F_w	$100 N$
return spring stiffness	$K_{1,2,3}$	$63000 N/m$
return spring mass	$M_{1,2,3}$	$.0227 kg$
return spring damping ratio	η_{rs}	.075
return spring damping	$C_{1,2,3}$	$\eta_{rs} 2\sqrt{M_1 K_1}$
cam eccentricity	e	$.01905 m$

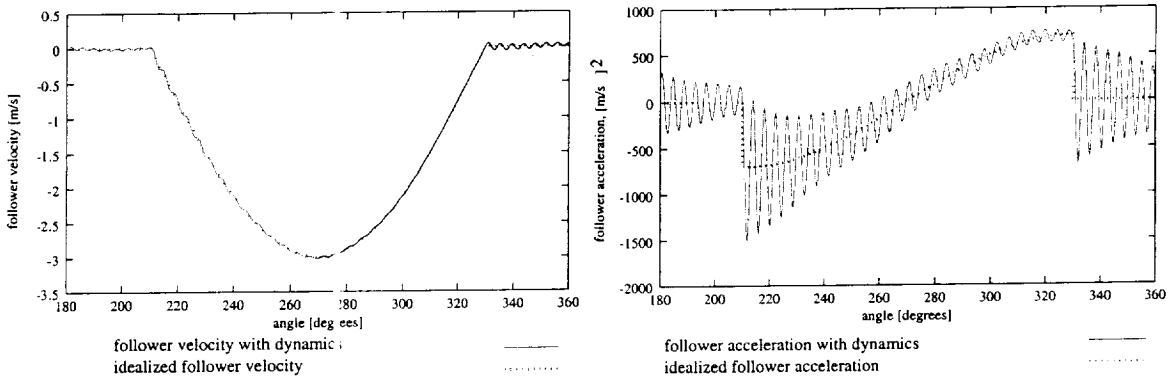

Figure 7: Follower velocity and acceleration per cam rotation with ideal cam surface smoothness and profile tolerance.

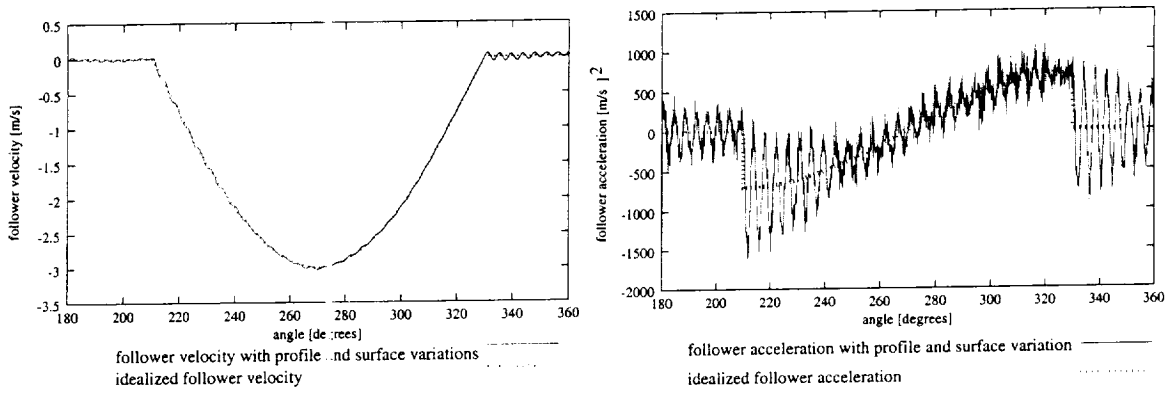

Figure 8: Follower velocity and acceleration per cam rotation with profile and surface variation on the cam.

and a surface roughness of 2.0 μm added to the cam profile. The profile error is modeled using a deterministic offset, simulated on the cam surface by the addition of a sinusoid of $t_p/3sin(n\theta)$. In this case, t_p is the profile tolerance and n was taken to be small compared to the forcing frequency (1500 RPM) and large with respect to the step size of the simulation code. The surface roughness is modeled using a random number generator and transformation techniques to simulate the surface roughness.

The addition of these geometric variations cause minimal change in follower velocity as a function of cam angle. However, the simulations show that a geometric variation in the cam causes a significantly different acceleration, with a large magnitude, in the follower The effective higher frequency and magnitude follower will cause significantly different vibrations on the system. Of particular relevance to our effort to simulate failure modes is that an increase in follower acceleration is related to an increase in the wear rate of the cam and follower (Rothbart, 1956). Also of key importance is that acceleration is generally the signal that is monitored for structural health status. Thus, the behavior of the acceleration signal is critical for accurate fault prediction and detection.

4 Probabilistic Cam-follower Vibration Model

Exploring the vibrational impact of variations in parameters such as spring stiffness provides a different simulation challenge. Parameter values of components vary from cam system to cam system, due to manufacturing and assembly variations. Because parts are replaced regularly during the lifecycle of systems, these variations are important to understand. For example, the spring constant on several cam systems can be distributed similarly to the distribution in Figure 5. In the end, vibration monitoring systems have to operate with generalized models of system response, with these types of variation included in such models.

The core research question is two-fold: 1) how much product variation results from a random fluctuation in the manufactured parts?; and, 2) how does response variation (e.g., vibration response distribution) relate to the parameters

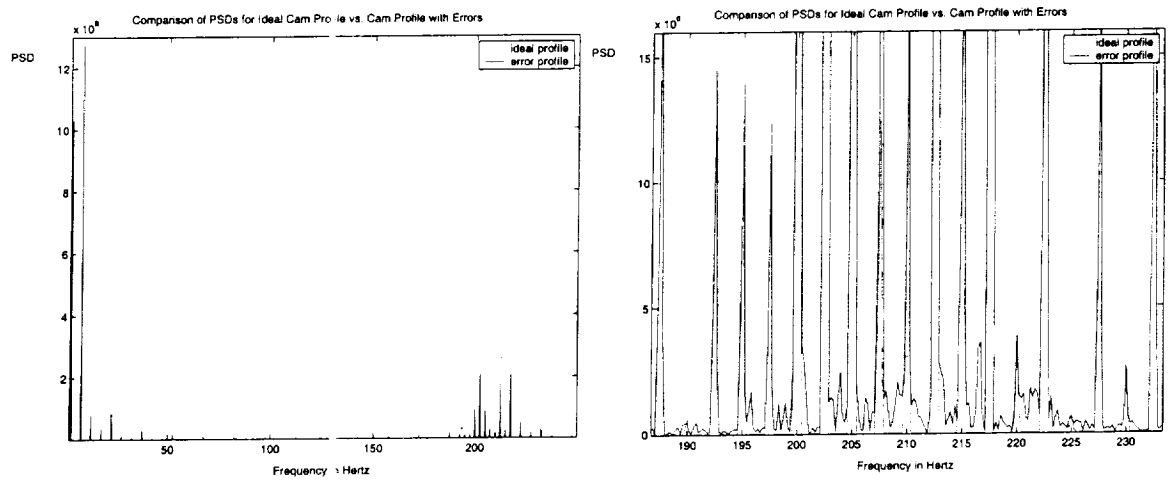

Figure 9: Comparison of Power Spectral Densities for an Ideal Cam Profile vs. a Cam with profile tolerance and surface roughness added (high-frequency range zoomed-in).

of a specific system being monitored? The answer to these questions will allow for a more informative design of vehicle health monitoring systems. For example, the behavior of some set of cam systems would be used to determine performance metrics, and windows on the metrics for acceptable performance. In this section, we explore the effect of a variation in spring stiffness (inherent from the manufacturing process) on a sampling of cam systems.

4.1 Analysis of Cam-Follower Vibration Signatures

Prior to analyzing the effect of design variations on the vibrational response, the vibration signature needs to be understood to decide on a possible set of features (vibration metrics) that will be used to monitor system performance and indicate the occurrence of failures. A small sample of the simulated cam-follower vibration responses is shown in Figures 7 and 8 for half a revolution (for an ideal cam and a cam with profile errors, respectively). 12 revolutions of these signals are used to analyze the frequency content, with a sampling frequency of $10,000\ Hz$ (the Nyquist cut-off frequency is $5,000\ Hz$.)

The frequency content of these signals is shown in Figure 9. The first plot shows the entire set of frequencies computed from the two signals. Based on a careful analysis, the only difference in the frequency content due to the addition of profile and surface errors manifests itself in the higher frequency range. The second plot shows a zoomed-in portion of the higher-frequency range where the difference due to the two signals can be seen clearly. In general, the addition of the profile and surface errors introduces frequencies in the noise range, as well as increasing the overall power levels.

Many possibilities exist for selecting a feature set for the purposes of monitoring changes in the vibration signatures (Smith, 1999; Lewicki and Coy, 1987; Tumer and Huff, 2001). In this paper, we first focus on the most most standard vibration monitoring feature, namely, the global measure of vibration levels. This measure can be computed as the area under the power spectral density plot in the frequency domain (equivalent to the variance in the time domain by Parseval's theorem.) Because most of the changes due to the addition of surface errors to the cam profile are observed in the higher-frequency range shown in Figure 9 ($\approx$ 177 Hz to 250 Hz), we select the total power in this range as the vibration metric of interest for this study.

4.2 Analysis of the Impact of Design Variations

The signals defined and analyzed in the previous subsection were varied using the Monte Carlo simulation method. In this case, both the signal from the ideal cam and from the cam with profile and surface errors are used to determine whether a random variation in the spring constants K_1, K_2, and K_3 (see model in Figure 6(b)), similar to the helical spring explored earlier, will result in variations in the vibration metric of interest (e.g., total power in the high-frequency range).

The spring constant tolerance model is developed by analogy with the earlier example in the paper. The spring constant mean is taken as 21,000 N/m with a standard deviation of 2.65% (660/17.5 = 0.0265) or 567 N/m. Recall that the spring that we explored before had a mean of 660 N/m and a standard deviation of 17.5 N/m. The spring was chosen as the element to vary because we can develop a reasonable tolerance model for this element (unlike the damping), and it is likely to have a larger effect on the vibrational response than one of the other parameters.

$N = 200$ number of trials are generated using the Monte Carlo simulation method (minimum number of trials required (Creveling, 1997)). A plot of the selected vibration metric is shown in Figure 10 for the case of the ideal cam profile and the cam profile with errors. As observed, the overall vibration levels and the variance in these levels are higher for the case of cam profile with errors.

The statistics (mean, standard deviation, skewness, kurtosis) of the vibration data generated using MC simulation are summarized in Table 2 for all of the frequency ranges for comparison. Using the high-frequency range once again, the ideal profile case results in a mean value of 62,967.00 and a standard deviation of 83.98, resulting in a tolerance of 251.95. The error profile case results in a mean value of 69,250.00 and a standard deviation of 3,468.50, resulting in a tolerance of 10,404.00 for the overall vibration metric.

Recall from the earlier review of Monte Carlo techniques that the standard approach to computing tolerances (using Equations 3 and 4) based on the complex mathematical relationship between the design parameters (d, G, D, and N) and the vibration response (sum of the total power in $\ddot{y}_3$) would have been intractable and highly simplistic (linearized.) This computational approach provides the vehicle monitoring system designer with the possible ranges of expected values of the vibration monitoring metric, based on the random variation in the selected subset of design parameters. Figure 11 shows the statistical distribution of the high-frequency vibration power values for both cases

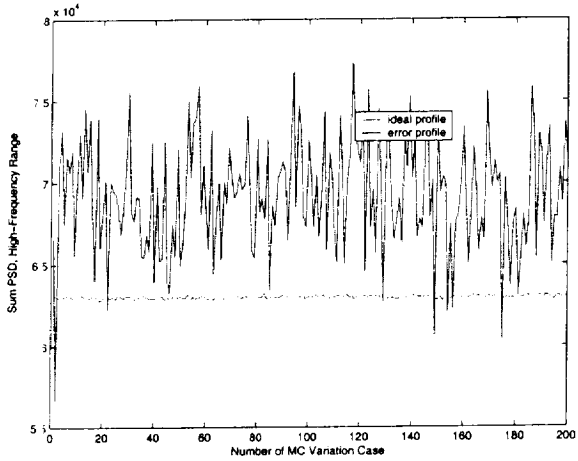

Figure 10: Total Power in the High-Frequency range for an Ideal Cam vs. a Cam with profile tolerance and surface roughness added.

Table 2: Statistics of Total Power Changes due to MC simulation.

	Ideal Profile				Error Profile			
Freq Range	Mean	St Dev	Skew	Kurt	Mean	St Dev	Skew	Kurt
Total	231670.00	82.51	-0.23	3.35	249930.00	3468.4	-0.25	3.15
Low-Freq	163880.00	0.54	-0.06	3.07	164120.00	143.27	-0.21	3.03
High-Freq	67967.00	83.98	-0.22	3.35	69250.00	3468.5	-0.25	3.18

(total number bins is 20.) As observed, the vibration metrics for both cases follow a normal distribution. However, the spread in the vibration metric computed from the case of cam profile with errors is much larger in value than the ideal cam profile case.

4.3 Discussion

Several observations can be made based on these analysis results. First, in addition to the mean levels of the vibration metric being larger, the variance in the value of the vibration metric due to the variation of the spring constant is larger (approximately a factor of 40) in the case of the cam with surface errors. This implies a greater impact of component variations on the vibration response of the (more realistic) cam with profile and surface errors. As a result, the models used for vehicle health monitoring systems not only have to take the variation in the design parameters into account, but also model the profile and surface errors more accurately, which is nonexistent from current models.

Second, the effect of the random variation in the spring constant (K) variable on the vibration metric is quite

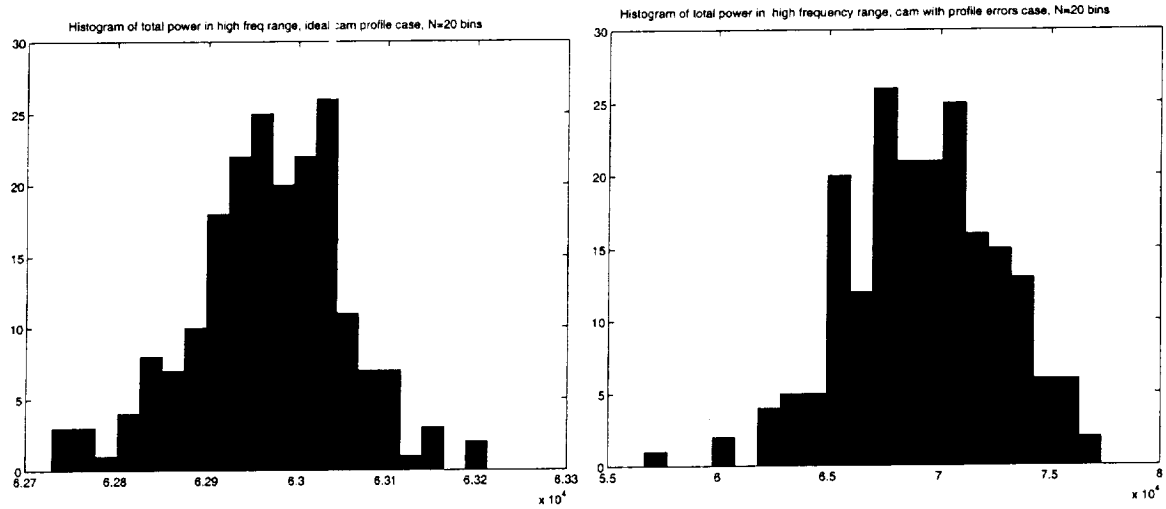

Figure 11: Histogram of the Probability Distribution of the Total Power in the High-Frequency range for an Ideal Cam vs. a Cam with profile tolerance and surface roughness added.

significant, as observed by the high variance value. The mathematical relationship describing the vibration metric selected in this study would have to be modified to add the expected variation which has propagated through the complex dynamic system, and resulted in the computed variation. In addition, the values of the metric within the computed variation range will have to be stored to assure the elimination of false alarms: in other words, training of the data must include the variation that has propagated through the system, so that anomalies are not identified incorrectly.

Let us revisit the situation described in Figure 1, where the four experimental factors (mast lift, mast bend, torque, and assembly) resulted in significant differences in vibration levels. The question those empirical observations brought up was whether any of these vibration levels were "acceptable". A probabilistic approach as described in this paper will enable the designer to set the limits of the vibration levels according to the mathematical model of the OH58 test rig vibrations, which will then identify which of the test conditions fall within the acceptable limits of variation. A similar approach can be followed for the situation described in Figure 2, where the vibration metric would be the power level at each of the frequencies, and angular variations in the placement of the planet gears can be propagated through the system to determine further effects.

5 Closure

This paper addresses the problem of incorrect modeling assumptions made when designing vehicle health monitoring systems, resulting in high rates of false alarms and missed detections. The specific problem that was addressed is the necessity of including the effect of statistical variations introduced during the design and manufacturing of rotating machinery components that make up most aerospace systems. The propagation of such significant variations through the system and their effect on the final monitoring metric of interest is typically unknown. In this paper, probabilistic methods (e.g., Monte Carlo simulation) are used to describe the nature of the variations in the system response due to variations in a subset of design parameters. The results show significant variation that must be taken into account using probabilistic models.

The paper presents an initial feasibility of enhancing deterministic dynamic models of complex systems by combining them with probabilistic models. Only a subset of design parameters (those describing the spring constant K) were considered in this paper. For a more thorough analysis, a full MC simulation is needed on all the parameters, followed by a sensitivity analysis. Furthermore, careful statistical tests need to be performed to determine the nature of the parameter distributions resulting from the MC simulation. Finally, the paper uses a simple cam-follower system. Future work will attack the problem of high-risk aerospace systems with much more complex system models. As demonstrated in this paper, the effect of surface and profile errors requires special attention in such complex system. Ongoing work focuses on developing finite difference models of rotorcraft transmission systems and aircraft engine gear systems. These models will be used to determine whether and how the design and manufacturing variations propagate through the systems, and how they can be represented in the signal modeling assumptions for vehicle health monitoring systems. Using this approach, variational models can be developed without reliance on systems that are simply expressed parametrically.

References

Creveling, C. (1997). *Tolerance design: a handbook for developing optimal specifications*. Prentice Hall PTR, New York, NY.

Eisen, M. (1969). *Introduction to Mathematical Probability Theory*. Prentice-Hall, Englewood Cliffs, New Jersey.

Grewal, P. S. and Newcombe, W. R. (1988). Dynamic performance of high-speed semi-rigid follower cam systems - effects of cam profile errors. *Mechanism and Machine Theory*, 23:121–133.

Hahn, G. J. and Shapiro, S. S. (1994). *Statistical Models in Engineering*. John Wiley and Sons, Inc., New York.

Hammersley, J. and Handscomb, D (1964). *Monte Carlo Methods*. Wiley, New York, NY.

Huff, E., Tumer, I., Barszcz, E., Dzwonczyk, M., and McNames, J. (2002). Analysis of maneuvering effects on transmission vibrations in an AH-1 Cobra helicopter. *Journal of the American Helicopter Society*, 47(1):42–49.

Huff, E., Tumer, I., Barszcz, E., Lewicki, D., and Decker, H. (2000). Experimental analysis of mast lifting and mast bending forces on vibration patterns before and after pinion reinstallation in an OH-58 transmission test rig. In *American Helicopter Society 56th Annual Forum*, Virginia Beach, VA.

Lewicki, D. and Coy, J. (1987). Vibration characteristics of OH58a helicopter main rotor transmission. *NASA Technical Paper*, NASA TP-2705/AVSCOM TR 86-C-42.

McAdams, D. A. and Wood, K. L. (1996). The effect of a fractal tolerance on the dynamic performance of cams. In *Proceedings of the ASME Design For Manufacturing Conference*, Irvine CA.

McAdams, D. A. and Wood, K. L. (2000). Tuning parameter tolerance design: Foundations, methods, and measures. *Research in Engineering Design*, 12(1):152–162.

Metropolis, N. and Ulam, S. (1949). The monte carlo method. *Journal of American Statistics*, 44(247):335–341.

Rothbart, H. A. (1956). *Cams: Design, Dynamics and Accuracy*. John Wiley & Sons, New York, New York.

Shigley, J. E. and Mischke, C. R. (2001). *Mechanical Engineering Design*. McGraw Hill, St. Louis, MO, 6th edition.

Smith, J. (1999). *Gear Noise and Vibration*. Marcel Dekker.

Tumer, I. and Huff, E. (2001). Using triaxial vibration data for monitoring of helicoper gearboxes. In *ASME Mechanical Vibration and Noise Conference*, volume DETC2001-VIB21755, Pittsburgh, PA.

Tumer, I. and Huff, E. (2002). On the effects of production and maintenance variations on machinery performance. *Journal of Quality in Maintenance Engineering*, To appear in September 2002.